Geochemical Perspectives Letters

Chondritic chlorine isotope composition of acapulcoites and lodranites

A. Stephant[1,2]*, M. Anand[2], C. Carli[1], X. Zhao[2], J. Davidson[3], T. Cuppone[4], G. Pratesi[4], I.A. Franchi[2]

OPEN ACCESS

https://doi.org/10.7185/geochemlet.2406

Abstract

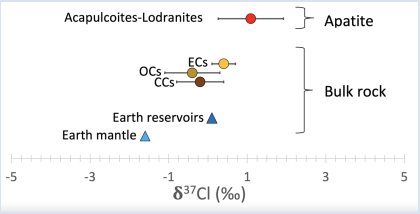

Bulk rock chondrites and Earth's reservoirs share a common chlorine isotopic value, while more differentiated bodies such as the Moon or Vesta record significant chlorine isotopic fractionation in their Ca phosphates. As such, an important but scarcely studied parameter is the effect of melting and differentiation processes on chlorine concentration and isotopic composition of a planetesimal. Here we report chlorine abundances and isotopic compositions for apatite in a range of primitive achondrites, acapulcoites and lodranites. These meteorites originated from a parent body that experienced some partial melting, allowing an assessment of chlorine behaviour during the early stages of planetary evolution in the inner Solar System. Overall, while bulk rock estimates of F and Cl abundances are indicative of degassing during the early stages of partial melting, no chlorine isotopic fractionation is recorded in apatite. Consequently, acapulcoites and lodranites retain their chondritic precursor isotopic signature for chlorine.

Received 2 October 2023 | Accepted 17 January 2024 | Published 16 February 2024

Introduction

Volatile elements are tracers of degassing processes experienced by planetesimals during thermal metamorphism and differentiation in the inner Solar System. Chlorine (Cl) is by far the most abundant halogen in chondritic meteorites, in the range of hundreds of $\mu g.g^{-1}$ in bulk samples (Brearley and Jones, 2018; Lodders and Fegley, 2023), while being depleted in the Earth compared to chondritic abundances (Dreibus *et al.*, 1979). Bulk chlorine isotope analyses of terrestrial mantle-derived samples originating from various mid-ocean ridges, together with sediments sampling the crust, have led to the observation that no isotopic fractionation of Cl occurred during the differentiation, and subsequent volatile loss, of the Earth (Sharp *et al.*, 2013). In addition, the bulk chlorine isotopic composition of enstatite (ECs), ordinary (OCs) and carbonaceous (CCs) chondrites are similar to those of terrestrial reservoirs, which also led to the inference of a chondritic origin for Earth's chlorine and the initial suggestion of a homogenous chlorine isotopic composition of the nebula, with a $\delta^{37}Cl$ value estimated at -0.3 ± 0.3 ‰ (Sharp *et al.*, 2013).

However, measurements of low chlorine isotopic compositions in a variety of extraterrestrial samples have challenged the chondritic/terrestrial $\delta^{37}Cl$ value to be representative of the nebula's primitive chlorine isotopic composition. Indeed, significant chlorine isotopic variations between the terrestrial mantle and surface reservoirs have been highlighted, the former recording a lower $\delta^{37}Cl$ value, from −1.6 to −4.0 ‰ (Bonifacie *et al.*, 2008; Layne *et al.*, 2009). The hypothesis of a low chlorine isotopic composition for the nebula has been further strengthened with even lower $\delta^{37}Cl$ values measured in a variety of meteoritic samples, down to −6 ‰ for Mars (Shearer *et al.*, 2018), −3.8 ‰ for eucrites (Sarafian *et al.*, 2017; Barrett *et al.*, 2019), −4.7 ‰ for the OC Parnallee (Sarafian *et al.*, 2017), and even down to −7.2 ‰ for iron meteorites (Gargano and Sharp, 2019). As a result, it is now suggested that the primitive chlorine composition of the nebula should have been close to −7.2 ‰; the higher $\delta^{37}Cl$ values observed denoting a later incorporation of ^{37}Cl-enriched HCl hydrates into accreting material in the case of chondrites or degassing processes for larger bodies (*e.g.*, Sharp *et al.*, 2013), although interaction with an HCl-rich ice impactor could have happened on differentiated bodies (Tartèse *et al.*, 2019).

The main carriers of chlorine in most meteorites are the three minerals belonging to the apatite group, namely hydroxyapatite, chlorapatite and fluorapatite, represented by the general formula $Ca_5(PO_4)_3(F,Cl,OH)$ (McCubbin and Jones, 2015). Therefore, in the following the term apatite will be used to refer generically to the three mineral species. Apatite is a volatile bearing Ca phosphate widespread in extraterrestrial samples and, as such, is key to investigate the distribution of volatile reservoir(s), in particular hydrogen and chlorine, in the inner Solar System, and to infer characteristics of the parent body from which they derive such as volatile depletion or differentiation (McCubbin *et al.*, 2023). *In situ* chlorine isotopic measurements in apatite by secondary ion mass spectrometry (SIMS) tend to show some

1. Istituto di Astrofisica e Planetologia Spaziali - INAF, Roma, Italy
2. School of Physical Sciences, The Open University, Milton Keynes, MK7 6AA, UK
3. Buseck Center for Meteorite Studies, School of Earth and Space Exploration, Arizona State University, Tempe, AZ 85287, USA
4. Dipartimento di Scienze della Terra, Università degli Studi di Firenze, Firenze, Italy
* Corresponding author (email: alice.stephant@inaf.it)

significant variability compared to bulk analyses performed either by gas source isotope ratio mass spectrometry (IRMS) or thermal ionisation mass spectrometry (TIMS) (Sharp *et al.*, 2013; Gargano *et al.*, 2020). The large ranges of δ^{37}Cl values measured in lunar and eucrite apatite have been interpreted as isotopic fractionation following metal chloride degassing during planetary differentiation (*e.g.*, Sharp *et al.*, 2010; Barnes *et al.*, 2019; Barrett *et al.*, 2019) and, in the case of the Moon, may not be representative of bulk rock δ^{37}Cl value (Gargano *et al.*, 2020). As such, effects of differentiation processes on chlorine isotopic composition in apatite, such as metamorphism and partial melting, have yet to be investigated.

In order to comprehend the processes responsible for δ^{37}Cl fractionation in apatite and the potential effect of parent body processes, in particular partial melting, we have investigated the chlorine abundances and isotopic compositions in phosphates from primitive achondrites, acapulcoites and lodranites. Acapulcoites and lodranites derive from a single partially differentiated parent body, and the chemical composition of its chondritic precursor lies between ordinary and enstatite chondrites (*e.g.*, Keil and McCoy, 2018; and references therein). These samples are strategic targets as they recorded a range in the degrees of planetary differentiation, from 1 % of partial melting for the less metamorphosed acapulcoites, some of which still retain relict chondrules, up to 20 % partial melting for the most differentiated lodranites, which have suffered from melt loss as evidenced by the depletion in plagioclases (*e.g.*, McCoy *et al.*, 1997). As such, these samples enable investigation of the role of thermal metamorphism and partial melting on the δ^{37}Cl composition of apatite in meteorites.

Materials and Methods

Three acapulcoites (Acapulco, NWA 10074, Dhofar 125) and two lodranites (Lodran and NWA 11970), covering 1 % to 20 % partial melting were investigated (see Supplementary Information for details on samples). Whole mount X-ray maps of Ca, Fe, Mg, P and Si were collected on the Cameca SX-100 electron probe microanalyser (EPMA) at the University of Arizona to identify phosphates in thin sections of Acapulco, NWA 10074, Dhofar 125, NWA 11970 and Lodran (Fig. S-1). Chemical characterisation of phosphates was carried out with a JEOL Superprobe JXA-8230 EPMA at the Department of Earth Sciences, University of Firenze. Chlorine concentration and isotopic measurements were performed with the secondary ion mass spectrometer NanoSIMS 50L at the Open University, UK. Secondary negative ions $^{1}H^{16}O^{-}$, $^{18}O^{-}$, $^{35}Cl^{-}$, $^{37}Cl^{-}$ and $^{40}Ca^{19}F^{-}$ were measured on 12 phosphates from Acapulco, NWA 10074 and Dhofar 125 (n = 21) using a Cs^{+} primary beam of ~10 pA rastered over a 5 μm × 5 μm surface area. These same negative ions were imaged by scanning mode over a 10 μm × 10 μm surface area for three phosphates in Lodran and Dhofar 125 (n = 4) <50 μm, too small for spot analyses. Unfortunately, no suitable phosphates for NanoSIMS analyses were found in NWA 11970, mainly due to the presence of cracks. Further details on the analytical protocol can be found in Supplementary Information (Figs. S-2 to S-4).

Phosphates in Acapulcoites-Lodranites: Petrographic Context and Volatile Abundances. Phosphates in acapulcoites and lodranites occur either as interstitial grains of fluorapatite or chlorapatite associated with Fe-Ni metal (Zipfel *et al.*, 1995) or in large veins (McCoy *et al.*, 1996). In fact, similarly to ordinary and carbonaceous chondrites, halogens have been concentrated in apatite almost entirely as a result of secondary processes such as thermal metamorphism (Brearley and Jones, 2018). Phosphorus contained within Fe-Ni metal diffuses out of the metal to form secondary phosphates as metamorphic grade increases (Jones *et al.*, 2014). Interestingly, apatite in OCs also contain low H_2O contents, <100 $\mu g.g^{-1}$ (Jones *et al.*, 2014), similar to the estimation of water abundances in acapulcoites, *i.e.* <50 $\mu g.g^{-1}$ (Stephant *et al.*, 2023). Jones *et al.* (2014) suggested that in OCs the apatite record the latest stages of fluid compositions, which were halogen-rich and water-poor. These fluids could have been derived by degassing of melts, produced either by partial melting in the interior of the ordinary chondrite parent bodies, or as a result of impact melting. As such, acapulcoites and lodranites could have recorded these fluids in their apatite, in a similar manner to the OCs.

In apatite, F–, Cl–, and hydroxyl (OH–) anions occupy the X crystallographic site. Cl contents measured by EPMA and by NanoSIMS present a good match, with NanoSIMS Cl abundances ranging from 0.48 ± 0.02 to 6.53 ± 0.33 wt. % (Fig. S-5). As such, we assume that X = F + Cl + OH and recalculated F abundance based on Cl and OH abundances, since F could be overestimated (Davidson *et al.*, 2020; McCubbin *et al.*, 2021; Supplementary Information). The acapulcoite-lodranite apatite compositions cover the entire chloro-fluor-apatite compositional range (Fig. 1). Apatite in acapulcoites Acapulco and NWA 10074 are all F-rich, with F contents >2.80 wt. %, that display mostly subhedral shapes associated with Fe-Ni metallic phases (Fig. S-2). Acapulco apatite are generally several hundreds of μm in size and have an average Cl content of 1.6 ± 0.12 wt. % (n = 5; 2 s.d.), while NWA 10074 apatite sizes range around 100 μm and are Cl-poor with Cl contents below 0.52 ± 0.01 wt. %. Dhofar 125 contains Cl-rich apatite with varying F concentrations (2.89–5.57 wt. % Cl; 0.69–2.26 wt. % F; Fig. 1) and have smaller grain sizes than in the other two acapulcoites (50–100 μm). In the two lodranites Lodran and NWA 11970, apatite is rarer and much smaller (20 to 50 μm). NWA 11970 phosphates are heavily fractured and thus are unsuitable for NanoSIMS analyses. Lodran apatite are all F-poor chlorapatite (6.17 ± 0.05 wt. % Cl) while NWA 11970 is mostly comprised of volatile-free merrillites, with only one F-rich chlorapatite found in the thin section (2.49 wt. % F; 2.44 wt. % Cl). The F-rich composition of most acapulcoite and lodranite apatite analysed here is similar to some OCs affected by impact melting (McCubbin *et al.*, 2023), as well as igneous apatite found in eucrites (*e.g.*, McCubbin *et al.*, 2021) and in lunar mare basalts (*e.g.*, Boyce *et al.*, 2014). Chondritic apatite are typically enriched in Cl (Brearley and Jones, 2018), similar to Lodran and Dhofar 125, suggesting latest stages of fluid compositions. However, it is important to note here that OC apatite also contain another unknown component, other than OH, missing in acapulcoite-lodranites (Jones *et al.*, 2014).

During degassing of its parental melt, apatite should evolve towards fluorapatite composition due to the relative volatility of the X site components: H > Cl > F (McCubbin *et al.*, 2021). Here, Lodran which underwent higher degrees of partial melting (*i.e.* 20 %; Supplementary Information), contain chlorapatite, which would tend to argue against preferential degassing of Cl towards F. However, considering that higher abundances of H and Cl should be released with increasing partial melt, the abundances of H, Cl and F in apatite cannot directly hint to the potential volatile loss experienced by these primitive achondrites during partial melting. As such, we need to estimate the bulk abundances of volatiles in acapulcoites and lodranites in order to gain insight into the behaviour of Cl, F and H abundances during early planetary differentiation.

Bulk Rock Abundances of F, Cl and H_2O in Acapulcoites and Lodranites. Using the method detailed in McCubbin *et al.* (2021), we estimated the bulk F abundance for each meteorite studied here, as well as their Cl and H_2O bulk abundances (Supplementary Information; Table S-2). Acapulcoites bulk F

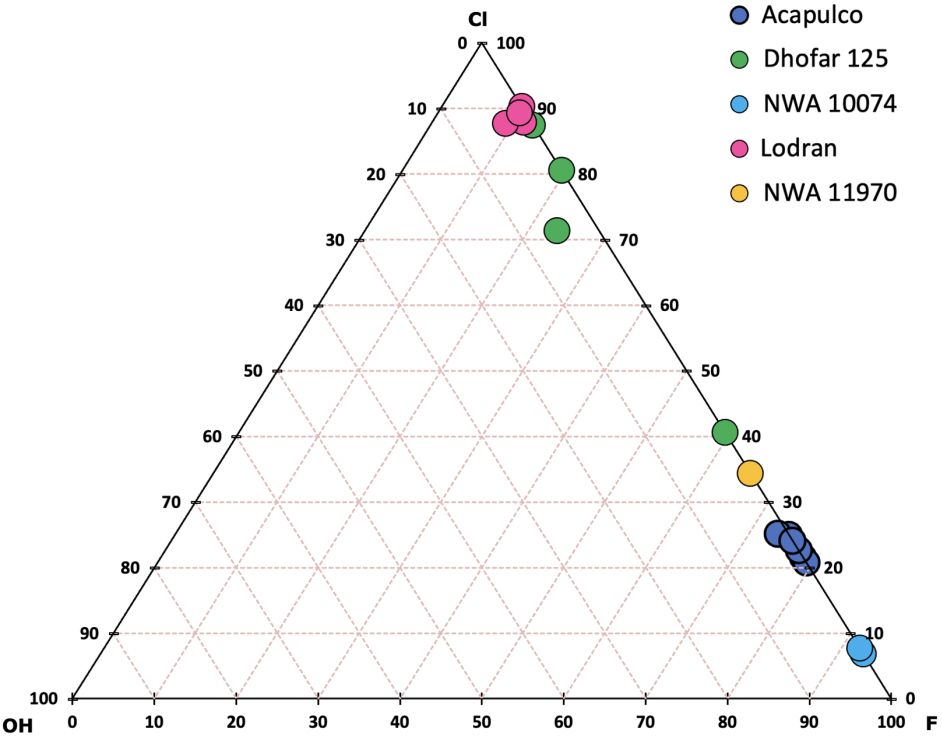

Figure 1 Ternary plot of apatite X-site occupancy (wt. %) from acapulcoites and lodranites. Procedures adopted for estimating OH and F contents are explained in the main text and Supplementary Information (McCubbin *et al.*, 2021).

abundances range from 42–392 $\mu g.g^{-1}$ while Lodran bulk F content is estimated to be 2 $\mu g.g^{-1}$. Bulk Cl concentrations have been estimated by McCoy *et al.* (1997) for Acapulco (*i.e.* 250 $\mu g.g^{-1}$) and Lodran (*i.e.* 10 $\mu g.g^{-1}$), as well as from Garrison *et al.* (2000) for Acapulco (*i.e.* 204 ± 26 $\mu g.g^{-1}$) with other acapulcoites ranging from 131 ± 38 to 268 ± 28 $\mu g.g^{-1}$ and lodranites from 35 ± 110 to 78 ± 69 $\mu g.g^{-1}$. Due to large uncertainties on the Cl, F and OH partition coefficient between melt and apatite (McCubbin *et al.*, 2015), we estimate lower limits for Cl bulk abundances. These estimations are in the range of literature data, ranging from 47 to 501 $\mu g.g^{-1}$ Cl for acapulcoites and from 59 to 73 $\mu g.g^{-1}$ Cl for lodranites. Depending on modal abundance estimations (see Supplementary Information), Dhofar 125 may have a higher bulk Cl content due to terrestrial alteration, highlighted by its higher degree of weathering (W1/W2) and the contiguous terrestrial alteration products to phosphates (Fig. S-2). Indeed, an increase of 0.4 vol. % of Ca phosphates in modal abundance estimation results in a bulk Cl abundance estimation almost three times higher. This highlights the necessity of precise Ca phosphate modal abundance in order to determine accurate bulk Cl abundances. Acapulcoites contain more F and Cl than lodranites, suggesting that lodranites experienced degassing or volatile-rich melt loss as a result of partial melting increase. Regarding the H_2O content, estimations based on apatite (*i.e.* 3–30 $\mu g.g^{-1}$ H_2O) are consistent with those made on nominally anhydrous minerals *via* NanoSIMS analyses (*i.e.* 3–19 $\mu g.g^{-1}$ H_2O; Stephant *et al.*, 2023). Overall, the bulk F and Cl contents of acapulcoite-lodranites are consistent with OC compositions (*i.e.* F = 8–300 $\mu g.g^{-1}$; Cl = 7–270 $\mu g.g^{-1}$; Lodders and Fegley, 2023 and references therein), while ECs are even more enriched in Cl (up to 1000 $\mu g.g^{-1}$; Brearley and Jones, 2018). As such, it would seem that the acapulcoites-lodranites still record the F and Cl contents of their chondritic precursor, which were very similar in composition to OC and EC parent bodies. Comparing the estimated volatile bulk content between acapulcoites and Lodran, it appears that Cl and F have either degassed or been carried away together with melt loss in lodranites, both mechanisms happening during early degree of partial melting (<20 %).

Effect of Partial Melting on the Chlorine Isotopic Composition of Phosphates. The $\delta^{37}Cl$ values in acapulcoite-lodranite apatite range from –0.91 ± 1.27 to +2.81 ± 0.71 ‰ (2 s.d.) (Table 1), with no apparent correlation with their large variation in Cl content (Fig. 2). Moreover, no correlation between $\delta^{37}Cl$ measured in a specific sample and its degree of partial melting is observed. As such, chlorine isotopic compositions of apatite in acapulcoites and lodranites do not record notable (<2 ‰) fractionation during partial melting. As a result, the average $\delta^{37}Cl$ value for acapulcoite-lodranites of +1.1 ± 0.8 ‰ (n = 25; 1 s.d.) is considered to be representative of the acapulcoite-lodranite parent body (ALPB), the chemical composition of which lies in between H ordinary chondrites and EL enstatite chondrites (*e.g.*, Keil and McCoy, 2018).

Sharp *et al.* (2013) measured bulk $\delta^{37}Cl$ values in OCs, ECs, and CCs, with values of –0.4 ± 0.7 ‰, +0.4 ± 0.3 ‰ and –0.2 ± 0.6 ‰, respectively (Fig. 2), arguing for no variation in chlorine isotopic composition amongst the different groups of chondrites. Taken at face value, the slightly heavier $\delta^{37}Cl$ of ALPB derived from apatite (+1.1 ± 0.8 ‰) could argue for some preferential loss of ^{35}Cl induced during metamorphism or degassing associated with partial melting. In fact, Sharp *et al.* (2013) also argued that the ~1 ‰ increase observed in bulk $\delta^{37}Cl$ between EH3 and EL6 chondrites could be interpreted as a sign of isotopic fractionation due to degassing. Moreover, the higher and more variable $\delta^{37}Cl$ values in apatite compared to bulk rock, also observed in lunar basalts, have been suggested to result from local degassing affecting apatite-forming melts and/or fluids (Gargano *et al.*, 2020). As a result, Gargano *et al.* (2020) suggested that lunar apatite are not representative of $\delta^{37}Cl$ bulk

Table 1 Cl content and δ^{37}Cl values and associated 2σ errors for apatite in Acapulco, NWA 10074, Dhofar 125 and Lodran measured by NanoSIMS (see Supplementary Information for details on the NanoSIMS protocol). Cl content estimated by EPMA is also given for comparison.

Sample	Phosphate number	Cl (wt. %)	2σ	δ^{37}Cl (‰)	2σ	Cl by EPMA (wt. %)
Acapulco	Ph1_2	1.61	0.08	0.96	0.81	1.49
	Ph1_3	1.64	0.08	1.42	0.81	1.49
	Ph2_2	1.64	0.08	0.46	0.82	1.44
	Ph2_3	1.62	0.08	0.06	0.83	1.44
	Ph3_2	1.74	0.09	1.33	1.27	1.72
	Ph3_3	1.71	0.09	−0.92	1.27	1.72
	Ph4_2	1.73	0.09	0.02	0.76	1.56
	Ph4_3	2.11	0.11	1.13	0.71	1.56
	Ph5_2	1.47	0.07	0.72	0.80	1.73
	Ph5_3	1.70	0.09	1.53	0.77	1.65
NWA 10074	Ph1-2	0.48	0.02	1.87	1.21	0.50
	Ph1_3	0.49	0.02	1.96	1.21	0.50
	Ph2_2	0.53	0.03	0.17	1.16	0.50
	Ph2_3	0.51	0.03	1.70	1.17	0.50
	Ph4_2	0.55	0.03	0.57	1.16	0.55
	Ph4_3	0.55	0.03	1.37	1.16	0.55
Dhofar 125	Ph1_1*	5.51	0.29	0.75	0.52	5.65
	Ph1_2*	6.05	0.32	1.57	0.51	5.65
	Ph2_2*	6.42	0.34	0.22	0.51	6.04
	Ph3_2	1.92	0.10	1.96	0.83	2.89
	Ph4_1	6.53	0.33	2.23	0.66	5.03
	Ph5_4	3.97	0.20	2.81	0.71	0.46
	Ph5_5	2.01	0.10	1.61	0.82	0.46
	Ph5_6	2.36	0.12	0.64	0.78	0.46
Lodran	Ph2*	5.44	0.28	1.02	0.51	6.18

* Identifies measurements made by image mode rather than spot mode.

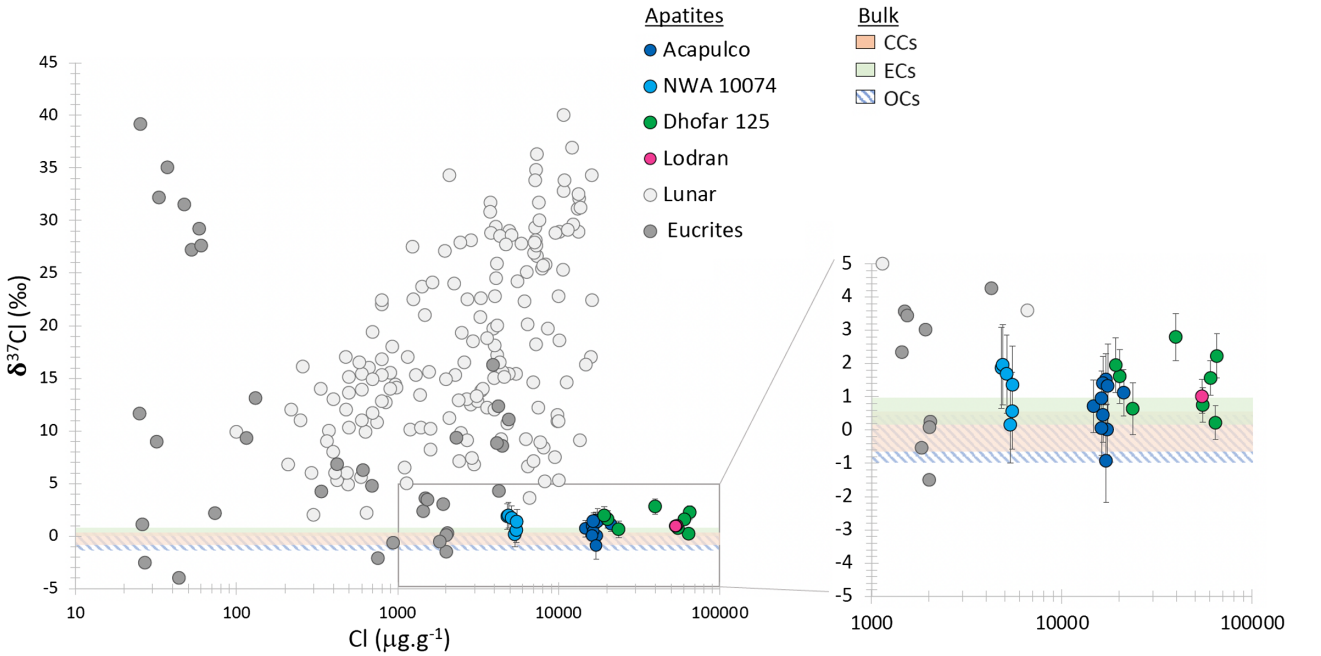

Figure 2 Chlorine abundance (µg.g^{-1}) and isotopic composition (δ^{37}Cl in ‰) of acapulcoite and lodranite apatite, lunar apatite (Barnes *et al.*, 2019 and references therein), eucrite apatite (Barrett *et al.*, 2019 and references therein). The orange band, green band and dashed blue band represent the average for bulk carbonaceous chondrites (CCs), enstatite chondrites (ECs) and ordinary chondrites (OCs), respectively (Sharp *et al.*, 2013).

rock. Nevertheless, our estimation of the ALPB δ^{37}Cl value is within uncertainties of δ^{37}Cl of bulk chondrites. Therefore, contrary to differentiated bodies, apatite in chondrites and primitive achondrites can be considered representative of their bulk Cl isotopic composition.

Conclusion

Overall, while some Cl and F degassing might have occurred at 20 % partial melting, as highlighted by the lower F and Cl contents estimated in Lodran, no significant chlorine isotopic fractionation among acapulcoite-lodranite apatite during early stages (*i.e.* lower degrees) of partial melting occurred. Therefore, acapulcoites and lodranites retain their chondritic δ^{37}Cl value, similar to that of most bulk chondrites. A similar conclusion has been reached regarding the hydrogen isotopic composition of acapulcoites and lodranites, where the δD value matches the inferred hydrogen isotopic composition of water in OCs (*cf.* Jin *et al.*, 2021; Stephant *et al.*, 2023). As such, it seems that acapulcoites and lodranites have retained most of their initial volatile chondritic isotopic compositions.

Acknowledgments

The authors would like to thank the Buseck Center for Meteorite Studies at Arizona State University for providing samples for this work. This manuscript was significantly improved by comments from two anonymous reviewers and the editorial expertise of Dr. Romain Tartèse. This work is supported by the EU's Horizon 2020 research and innovation programme under the Marie Skłodowska-Curie grant agreement no. 884029 to AS. This project has also received funding from the European Union's Horizon 2020 research and innovation programme under grant agreement no. 871149 to access the Open University NanoSIMS through the EuroPlanet programme (award code 20-EPN2-01). JD was supported by BCMS. CC, GP, and TC were partially supported by ASI INAF/ASI agreement no. 2018-16-HH.0, Ol-BODIES project. MA and IAF acknowledge funding from the UK Science and Technology Facilities Council (STFC) (#ST/X001180/1 #ST/T000228/1)

Editor: Romain Tartèse

Additional Information

Supplementary Information accompanies this letter at https://www.geochemicalperspectivesletters.org/article2406.

Cite this letter as: Stephant, A., Anand, M., Carli, C., Zhao, X., Davidson, J., Cuppone, T., Pratesi, G., Franchi, I.A. (2024) Chondritic chlorine isotope composition of acapulcoites and lodranites. *Geochem. Persp. Let.* 29, 14–19. https://doi.org/10.7185/geochemlet.2406

References

Barnes, J.J., Franchi, I.A., McCubbin, F.M., Anand, M. (2019) Multiple volatile reservoirs on the Moon revealed by the isotopic composition of chlorine in lunar basalts. *Geochimica Cosmochimica Acta* 266, 144–162. https://doi.org/10.1016/j.gca.2018.12.032

Barrett, T.J., Barnes, J.J., Anand, M., Franchi, I.A., Greenwood, R.C., Charlier, B.L.A., Zhao, X., Moynier, F., Grady, M.M. (2019) Investigating magmatic processes in the early Solar System using the Cl isotopic systematics of eucrites. *Geochimica Cosmochimica. Acta* 266, 582–597. https://doi.org/10.1016/j.gca.2019.06.024

Bonifacie, M., Jendrzejewski, N., Agrinier, P., Humler, E., Coleman, M., Javoy, M. (2008) The chlorine isotope composition of the Earth's mantle. *Science* 319, 1518–1520. https://doi.org/10.1126/science.1150988

Boyce J.W., Tomlinson S.M., McCubbin F.M., Greenwood J.P., Treiman A.H. (2014) The Lunar Apatite Paradox. *Science* 344, 400–402. https://doi.org/10.1126/science.1250398

Brearley, A.J., Jones, R.H. (2018) Halogens in Chondritic Meteorites. In: Harlov, D.E., and Aranovich, L. (Eds.) *The Role of Halogens in Terrestrial and Extraterrestrial Geochemical Processes*, Springer, 871–958. https://doi.org/10.1007/978-3-319-61667-4_15

Davidson, J., Wadhwa, M., Hervig, R.L., Stephant, A. (2020) Water on Mars: Insights from apatite in regolith breccia Northwest Africa 600 7034. *Earth and Planetary Science Letters* 552, 116597. https://doi.org/10.1016/j.epsl.2020.116597

Dreibus, G., Spettel, B., Wänke, H. (1979) Halogens in meteorites and their primordial abundances. *Physics and Chemistry of the Earth* 11, 33–38. https://doi.org/10.1016/0079-1946(79)90005-3

Gargano, A., Sharp, Z. (2019) The chlorine isotope composition of iron meteorites: Evidence for the Cl isotope composition of the solar nebula and implications for extensive devolatilization during planet formation. *Meteoritics and Planetary Science* 54, 1619–1631. https://doi.org/10.1111/maps.13303

Gargano, A., Sharp, Z., Shearer, C., Simon, J.I., Halliday, A., Buckley, W. (2020) The Cl isotope composition and halogen contents of Apollo-return samples. *Proceeding of the National Academy of Sciences USA* 117, 23418–23425. https://doi.org/10.1073/pnas.2014503117

Garrison, D., Hamlin, S., Bogard, D. (2000) Chlorine abundances in meteorites. *Meteoritics and Planetary Science* 35, 419–429. https://doi.org/10.1111/j.1945-5100.2000.tb01786.x

Jin, Z., Bose, M., Lichtenberg, T., Mulders, G.D. (2021) New Evidence for Wet Accretion of Inner Solar System Planetesimals from Meteorites Chelyabinsk and Benenitra. *Planetary Sciences Journal* 2, 244. https://doi.org/10.3847/PSJ/ac3d86

Jones, R.H., McCubbin, F.M., Dreeland, L., Guan, Y.B., Burger, P.V., Shearer C.K. (2014) Phosphate minerals in LL chondrites: A record of the action of fluids during metamorphism on ordinary chondrite parent bodies. *Geochimica Cosmochimica Acta* 132, 120–140. https://doi.org/10.1016/j.gca.2014.01.027

Keil, K., McCoy, T.J. (2018) Acapulcoite-lodranite meteorites: Ultramafic asteroidal partial melt residues. *Geochemistry* 78, 153–203. https://doi.org/10.1016/j.chemer.2017.04.004

Layne, G.D., Kent, A.J.R., Bach, W. (2009) δ^{37}Cl systematics of a backarc spreading system: the Lau Basin. *Geology* 37, 427–430. https://doi.org/10.1130/G25520A.1

Lodders, K., Fegley Jr., B. (2023) Solar system abundances and condensation temperatures of the halogens fluorine, chlorine, bromine, and iodine. *Geochemistry* 83, 125957. https://doi.org/10.1016/j.chemer.2023.125957

McCoy, T.J., Keil, K., Clayton, R.N., Mayeda, T.K., Bogard, D.D., Garrison, D.H., Huss, G.R., Hutcheon, I.D., Wieler, R. (1996) A petrologic, chemical, and isotopic study of Monument Draw and comparison with other acapulcoites: Evidence for formation by incipient partial melting. *Geochimica et Cosmochimica Acta* 60, 2681–2708. https://doi.org/10.1016/0016-7037(96)00109-3

McCoy, T.J., Keil, K., Muenow, D.W., Wilson, L. (1997) Partial melting and melt migration in the acapulcoite-lodranite parent body. *Geochimica et Cosmochimica Acta* 61, 639–650. https://doi.org/10.1016/S0016-7037(96)00365-1

McCubbin, F.M., Jones, R.H. (2015) Extraterrestrial apatite: Planetary geochemistry to astrobiology. *Elements* 11, 183–188. https://doi.org/10.2113/gselements.11.3.183

McCubbin, F.M., Vander Kaaden, K.E., Tartèse, R., Boyce, J.W., Mikhail, S., Whitson, E.S., Bell, A.S., Anand, M., Franchi, I.A., Wang, J.H., Hauri, E.H. (2015) Experimental investigation of F, Cl, and OH partitioning between apatite and Fe-rich basaltic melt at 1.0-1.2 GPa and 950-1000 °C. *American Mineralogist* 100, 1790–1802. https://doi.org/10.2138/am-2015-5233

McCubbin, F.M., Lewis, J.A., Barnes, J.J., Elardo, S.M., Boyce J.W. (2021) The abundances of F, Cl, and H_2O in eucrites: Implications for the origin of volatile depletion in the asteroid 4 Vesta. *Geochimica et Cosmochimica Acta* 314, 270–293. https://doi.org/10.1016/j.gca.2021.08.021

McCubbin, F.M., Lewis, J.A., Barnes, J.J., Boyce, J.W., Gross, J., McCanta, M.C., Srinivasan, P., Anzures, B.A., Lunning, N.G., Elardo, S.M., Keller, L.P., Prissel, T.C., Agee, C.B. (2023) On the origin of fluorine-poor apatite in chondrite parent bodies. *American Mineralogist* 108, 1185–1200. https://doi.org/10.2138/am-2022-8623

Sarafian, A.R., John, T., Roszjar, J., Whitehouse, M.J. (2017) Chlorine and hydrogen degassing in Vesta's magma ocean. *Earth and Planetary Science Letters* 459, 311–319. https://doi.org/10.1016/j.epsl.2016.10.029

Sharp, Z.D., Shearer, C.K., McKeegan, K.D., Barnes, J.D., Wang, Y.Q. (2010) The Chlorine Isotope Composition of the Moon and implications for an anhydrous mantle. *Science* 329, 1050–1053. https://doi.org/10.1126/science.1192606

Sharp, Z.D., Mercer, J.A., Jones, R.H., Brearley, A.J., Selverstone, J., Bekker, A., Stachel, T. (2013) The chlorine isotope composition of chondrites and Earth. *Geochimica Cosmochimica Acta* 107, 189–204. https://doi.org/10.1016/j.gca.2013.01.003

Shearer, C.K., Messenger, S., Sharp, Z.D., Burger, P.V., Nguyen, A.N., McCubbin, F.M. (2018) Distinct chlorine isotopic reservoirs on Mars. Implications for character, extent and relative timing of crustal interactions with mantle-derived magmas, evolution of the martian atmosphere, and the building blocks of an early Mars. *Geochimica Cosmochimica Acta* 234, 24–36. https://doi.org/10.1016/j.gca.2018.04.034

Stephant, A., Zhao, X., Anand, M., Davidson, J., Carli, C., Cuppone, T., Pratesi, G., Franchi, I.A. (2023) Hydrogen in acapulcoites and lodranites: A unique source of water for planetesimals in the inner Solar System. *Earth and Planetary Science Letters* 615, 118202. https://doi.org/10.1016/j.epsl.2023.118202

Tartèse, R., Anand, M., Franchi, I.A. (2019) H and Cl isotope characteristics of indigenous and late hydrothermal fluids on the differentiated asteroidal parent body of Grave Nunataks 06128. *Geochimica et Cosmochimica Acta* 266, 529–543. https://doi.org/10.1016/j.gca.2019.01.024

Zipfel, J., Palme, H., Kennedy, A.K., Hutcheon, I.D. (1995) Chemical composition and origin of the Acapulco meteorite. *Geochimica et Cosmochimica Acta* 59, 3607–3627. https://doi.org/10.1016/0016-7037(95)00226-P

Geochemical Perspectives Letters

Chondritic chlorine isotope composition of acapulcoites and lodranites

A. Stephant, M. Anand, C. Carli, X. Zhao, J. Davidson, T. Cuppone, G. Pratesi, I.A. Franchi

Supplementary Information

The Supplementary Information includes:

- Sample description
- Mineralogical and petrological analyses
- Chlorine abundance and isotopic composition analyses
- Tables S-1 and S-2
- Figures S-1 to S-5
- Supplementary Information References

Sample description

Acapulco

Acapulco fell on August 11, 1976 in Mexico and was first studied by Christophe Michel-Levy and Lorin (1978). In addition to being a fall, Acapulco is relatively unshocked (S1) (Palme *et al.,* 1981), similar to many other acapulcoites and lodranites. Acapulco is mostly composed of silicate minerals: olivine (25.1 vol. %), pyroxene, mostly as orthopyroxene (44 vol. %), feldspar (15 vol. %) (Yugami *et al.,* 1998). Using XMapTools 4.1 (Lanari *et al.,* 2014; 2019; 2023), we recalculated similar modal abundances for Acapulco (vol. %): 27.3 of olivine, 50.1 of orthopyroxene, 0.3 of clinopyroxene, 9.8 of feldspar, 10.9 of metallic phases and 1.6 of Ca-phosphates. Zipfel *et al.* (1995) reported no zoning in MgO and FeO in these silicates, consistent with this sample probably being the most equilibrated acapulcoite (McCoy *et al.,* 1996). Acapulco yields a higher metamorphism temperature than type 5–6 ordinary chondrites (Zipfel *et al.,* 1995), with an estimated temperature of 1170 °C (McCoy *et al.,* 1996; Palme *et al.,* 1981). McCoy *et al.* (1997b) estimated that Acapulco suffered from less than 1 % partial melting. In Acapulco, apatite is much more abundant than merrillite. A vein of Cl-F-bearing apatite in Acapulco was 1.8 mm *vs*. 200 microns in size (McCoy *et al.,* 1996).

NWA 10074

Northwest Africa (NWA) 10074 is an acapulcoite classified in 2014. It shows a recrystallized texture, with polygonal and subhedral grains typically <0.3 mm, with occasional larger (to 1 mm) grains of orthopyroxene. Silicates have homogenous compositions and represent 90 vol. % of the sample but no

precise modal abundances have yet been reported. We estimated modal abundances as follow (vol. %): 28.4 of olivine, 40.5 of orthopyroxene, 4.5 of clinopyroxene, 14 of feldspar, 7 of metallic phases and 0.5 of Ca-phosphates. The shock and weathering grades of this sample are low.

Dhofar 125

Dhofar 125 is another acapulcoite, found in 2000 in the Oman desert. Dhofar 125 is moderately weathered (W1) in the interior core of the rock, while slightly more weathered (W2) towards the edges. As for other acapulcoites, Dhofar 125 is dominated by orthopyroxene (35.6 vol. %), olivine (27.5 vol. %), feldspar (14 vol. %) and clinopyroxene (6.5 vol. %) (Greyshake *et al.,* 2001). Recalculated modal abundances using XMapTools 4.1 are consistent with these previous estimations (vol. %): 28.4 of olivine, 36.5 of orthopyroxene, 6.1 of clinopyroxene, 5.9 of feldspar, 22.5 of metallic phases and 0.3 of Ca-phosphates. The meteorite is also unshocked, similar to most other acapulcoites and lodranites, with olivine showing sharp extinction and few irregular fractures. Dhofar 125 also shows recrystallized texture with abundant 120° triple junctions (Patzer *et al.,* 2004), but its average grain size (97.3 μm) is slightly smaller than typical acapulcoites. Its equilibration temperature has been estimated at 1120 °C (Patzer *et al.,* 2004).

Lodran

Lodran fell in 1868 in Pakistan and is also unshocked (Sl) (McCoy *et al*., 1997a). Conversely to Acapulco, Lodran exhibits evidence for more than 20% of partial melting (Papike *et al.,* 1995). Based on the modal abundance data of Davis *et al.* (1993), Lodran is comprised of 53 vol. % of olivine and 47 vol. % of orthopyroxene, with some trace of chromite. Our thin section sample contains some large blebs of Fe-Ni metal compared to the one studied by Davis *et al.* (1993). Using XMapTools 4.1, we recalculated the modal abundances of Lodran (vol. %): 41.3 of olivine, 36.4 of orthopyroxene, 22.2 of metallic phases and 0.07 of Ca-phosphates.

NWA 11970

Northwest Africa 11970 was classified in 2016 as one of the few lodranite breccias. This material is likely paired with NWA 8118, NWA 8216, and NWA 8251. The weathering grade is also very low. Observations from a thin section show a breccia dominated by angular to sub-rounded silicate grains of which the largest grain is 1 cm long. Mineralogy is dominated by olivine, ortho- and clinopyroxenes. Estimations from XMapTools give modal abundances (vol. %) of 48.7 of olivine, 18.7 of clinopyroxene, 26.1 of orthopyroxene, 0.1 of phosphates and 6.9 of metallic phases.

Mineralogical and petrological analyses

Backscattered electron (BSE) images were obtained on polished thin sections of acapulcoites and lodranites loaned from the Buseck Center for Meteorite Studies (BCMS). Elemental X-ray maps of Ca, Fe, Mg, P and Si were collected on the Cameca SX-100 electron probe microanalyser (EPMA) at University of Arizona to identify Ca-phosphates in thin sections of Acapulco, NWA 10074, Dhofar 125, Lodran and NWA 11970 (Fig. S-1). Chemical characterisation of Ca-phosphates in these thin sections, performed after NanoSIMS analyses to avoid devolatilization, was carried out with a JEOL Superprobe JXA-8230 EMPA at the Department of Earth Sciences, University of Firenze. Quantitative analyses of Ca-phosphates were performed in wavelength dispersive mode, with an accelerating potential of 15 kV. A focused beam of 20 nA with a 3 μm spot size was used. ZAF correction was applied to all measurements. Typical detection limits were 0.02–0.05 % for major element oxide abundances. Standards used for these analyses are: albite astimex for Na, apatite astimex for P and Ca, fluorine

astimex for F, celestite astimex for Sr, tugtupite astimex for Cl, ilmenite from the Smithsonian for Fe, olivine astimex for Mg. Crystals for element detection were TAP for Na and Mg, PET for P, Sr, Cl and Ca, LIF for Fe and LDE1 for F. As F−, Cl−, and hydroxyl (OH−) anions occupy the X crystallographic site, Cl and F concentrations were corrected for apatite stoichiometry assuming $2 = X_F + X_{Cl} + X_{OH}$, following the method of Ketcham (2015). Since these Ca-phosphates are dry (<50 $\mu g.g^{-1}$ H_2O) (Stephant *et al*., 2023) and that Cl contents measured by NanoSIMS and by EPMA are consistent, it is most likely that F content by EPMA is overestimated, as also suggested by McCubbin *et al.* (2021). The chemical compositions of Ca-phosphates are presented in supplementary Table S-1. Modal abundances and estimation of bulk F, Cl and H_2O abundances in the studied samples following the method described in McCubbin *et al.* (2021) is provided in supplementary Table S-2.

Chlorine abundance and isotopic composition analyses

Chlorine abundances and Cl-isotopic compositions of 15 apatite were measured using the Cameca NanoSIMS 50L at the Open University, UK using a protocol modified after Tartèse *et al.* (2014), Barnes *et al.* (2016) and Barrett *et al.* (2019) following two modes: spot analyses for larger apatite grains found in Acapulco, NWA 10074 and Dhofar 125 (Ph3, Ph4 and Ph5) and imaging for grains which were less than 50 µm diameter in Lodran, NWA 11970 and Dhofar 125 (Ph 1 and Ph2) (cf. Supplementary Fig. S-2). For spot analyses, $^{1}H^{16}O$, ^{18}O, ^{35}Cl, ^{37}Cl, $^{40}Ca^{19}F$ secondary ions were measured using a Cs^+ primary beam of 10 pA rastered over 5 µm × 5 µm surface area. Each analysis surface area was divided into 64 × 64 pixels, with a counting time of 0.132 ms per pixel. The number of cycles was set at 800. Three minutes of pre-sputtering was set-up before analysis on a larger area (7 µm × 7 µm) than the analysed surface to remove any contamination from the surface and establish sputter equilibrium. An electron flood gun was used for charge compensation. $^{40}Ca^{19}F$ secondary ions were used to monitor that the spot was within the apatite. For image mode, the same secondary negative electrons were imaged by scanning ion imaging. Analyses were carried out using a Cs^+ primary current of 10 pA that was rastered over the sample on areas of 10 µm × 10 µm. Each analysis surface area was divided into 128 ×128 pixels, with a counting time of 1 ms per pixel. The number of cycles was set at 100. Pre-sputtering (15 µm × 15 µm) was also set-up before analysis, as well as the use of the electron flood gun. Images were processed with the L'IMAGE software developed by Larry Nittler from the Carnegie Institute of Washington (now Arizona State University). The deadtime was set at 44 ns and corrected with the L'IMAGE software. Regions of interest (ROIs) were determined on each image based on the $^{35}Cl/^{18}O$ and $^{40}Ca/^{18}O$ images to locate the apatite and exclude any cracks, voids or anomalously Cl-rich hotspots associated with extraneous contamination.

For both sets of analyses, terrestrial apatite standards Ap 004, Ap 005 and Ap 018 were used for relative sensitivity factor of Cl abundance (McCubbin *et al.,* 2012). Cl abundances were calibrated using the measured $^{35}Cl/^{18}O$ ratios and the known Cl abundances of terrestrial apatite standards (Fig. S-3). Uncertainties reported on Cl contents combine the 2σ analytical uncertainties associated with each individual measurement and the uncertainty associated with the calibration line. The good match between NanoSIMS and EPMA Cl content values give credit to the accuracy of our NanoSIMS analyses (Fig. S-4).

For Cl isotope measurements, the instrumental mass fractionation (IMF) factor, α, based on analyses of Ap 005 was 1.028 ± 0.001 (2s.d.) for spot analyses and 1.016 ± 0.001 (2s.d.) for image mode.

Reproducibility of $\delta^{37}Cl$ measurements on Ap 005 standard is presented in Figure S-4. The measured $^{37}Cl/^{35}Cl$ ratios are corrected for the IMF and expressed in $\delta^{37}Cl$ notation as defined in equation (Eq. S-1), with standard mean ocean chloride $\delta^{37}Cl_{SMOC}=0$ (Kaufman *et al.*, 1984).

$$\delta^{37}Cl\ (‰) = [(^{37}Cl/^{35}Cl_{sample})/(^{37}Cl/^{35}Cl_{SMOC})–1] \times 1000 \quad \text{(Eq. S-1)}$$

Weighted average of Ap 004 $\delta^{37}Cl$, corrected from IMF, is 0.27 ± 0.23 ‰ (N=33), consistent with its published value of 0.11 ‰ (McCubbin *et al.,* 2012). Errors estimated for $\delta^{37}Cl$ values take into consideration the error based on counting statistics, as well as the uncertainty associated with the IMF calculation. BSE images of analysed apatite and optical images of NanoSIMS spots can be found in Figure S-5.

Supplementary Tables

Table S-1 Chemical composition of apatite and merrillites in Acapulco, NWA 10074, Dhofar 125, Lodran and NWA 11970. Merri. Stands for merrillite. Data were processed using the "approach 1" template in Ketcham (2015). We assume that OH = 2 – (X_F and X_{Cl}) when the sum of X_F and X_{Cl} was below 2. When the sum of X_F and X_{Cl} exceeds 2 afu, F was computed assuming $X_F = 2 – X_{Cl}$. This is because F can be overestimated by EMPA (Davidson *et al.,* 2020; McCubbin *et al*., 2021), as highlighted by the fit between Cl abundance measured by EPMA and SIMS (cf. Figure S-5). Table S-1 (.xlxs) is available for download from the online version of this article at https://doi.org/10.7185/geochemlet.2406

Table S-2 Modal abundances of Acapulco, NWA 10074, Dhofar 125 and Lodran, from literature and this study, with the estimation of bulk F, H_2O and Cl abundances, based on the partition coefficient between melt and apatite of F, Cl and OH from McCubbin *et al.* (2015) and the method described in McCubbin *et al.* (2021). Apatite H_2O contents from Stephant *et al. (*2023) were used to calculate H_2O /F ratios. Literature data are given for comparison.

	Acapulco		NWA 10074	Dhofar 125		Lodran
Olivine	25.2	27.3	28.4	27.5	28.5	41.28
High-Ca pyroxene	2.5	0.3	4.5	6.5	6.1	
Low-Ca pyroxene	41.1	50.1	40.5	35.6	36.7	36.44
Plagioclase	14.8	9.8	14	14	5.9	
Chromite	0.8	-		0.5	-	
Ca-phosphate	1.2	1.6	0.5	0.7	0.3	0.07
Troilite	8.7	-	7	7.7	-	
Metal	5.7	10.9	3	5.3	22.5	22.21
Total	100.0	100	97.9	97.8	99.9	100
Reference	*Yugami et al. (1998)*	*This study*	*This study*	*Greyshake et al. (2001)*	*This study*	*This study*

Table S-2 continued	Acapulco		NWA 10074	Dhofar 125		Lodran
F wt.% in apatite	2.82 ± 0.09		3.55 ± 0.14	0.69 ± 0.22 (75% of apatite) 2.26 (25% of apatite)		0.37 ± 0.03
F bulk rock (mg.g^{-1}) this study	**308**	**392**	**171**	**71**	**42**	**2**
error	**±10**	**±10**	**±10**	**±10**	**±10**	**±0.1**
H_2O/F	0.037 - 0.077		0.015 - 0.052	0.180		
Cl/F	0.98 - 1.28		0.28 - 0.32	2.56 – 26.34		29.43 – 36.25
H_2O bulk (µg.g^{-1}) this study	**11-24**	**14 - 30**	**03-09**	**< 27**	**< 9**	
H_2O bulk (µg.g^{-1}) (Stephant *et al.*, 2023)	03-09		06-18	05-14		18 - 31
Cl bulk (µg.g^{-1}) lower limits - this study	**302 - 394**	**384 - 501**	**47 - 54**	**374 – 1185**	**131-421**	**59- 73**
Cl bulk (µg.g^{-1}) (McCoy *et al.*, 1997b)	250					10
Cl bulk (µg.g^{-1}) (Garrison *et al.*, 2000)	204 ± 246		131 - 268*	131 - 268*		35 - 78*

* range of average values

Supplementary Figures

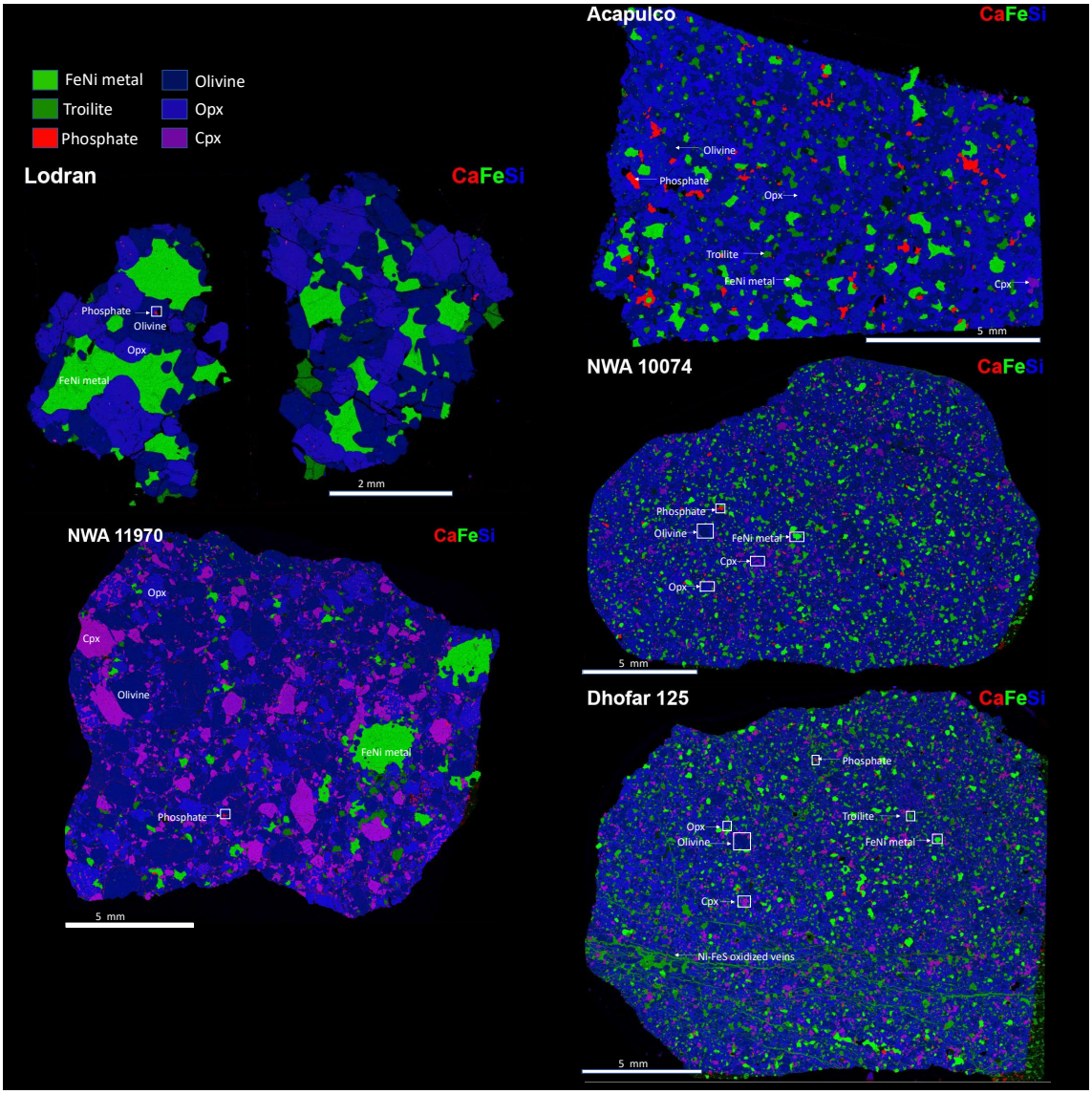

Figure S-1 Composite X-ray maps of Acapulco, NWA 10074, Dhofar 125, Lodran and NWA 11970 showing the distribution of FeNi metal, troilite, olivine, orthopyroxene (opx), clinopyroxene (cpx) and Ca-phosphates. Ca-phosphates in acapulcoites are generally associates with FeNi metal, while they are bounded to silicates in lodranites. Acapulco exhibit large grains of apatite of a few hundreds of microns, while acapulcoite apatite size range from 50 to 200 microns. Lodranites display apatite grains smaller than 50 microns in size.

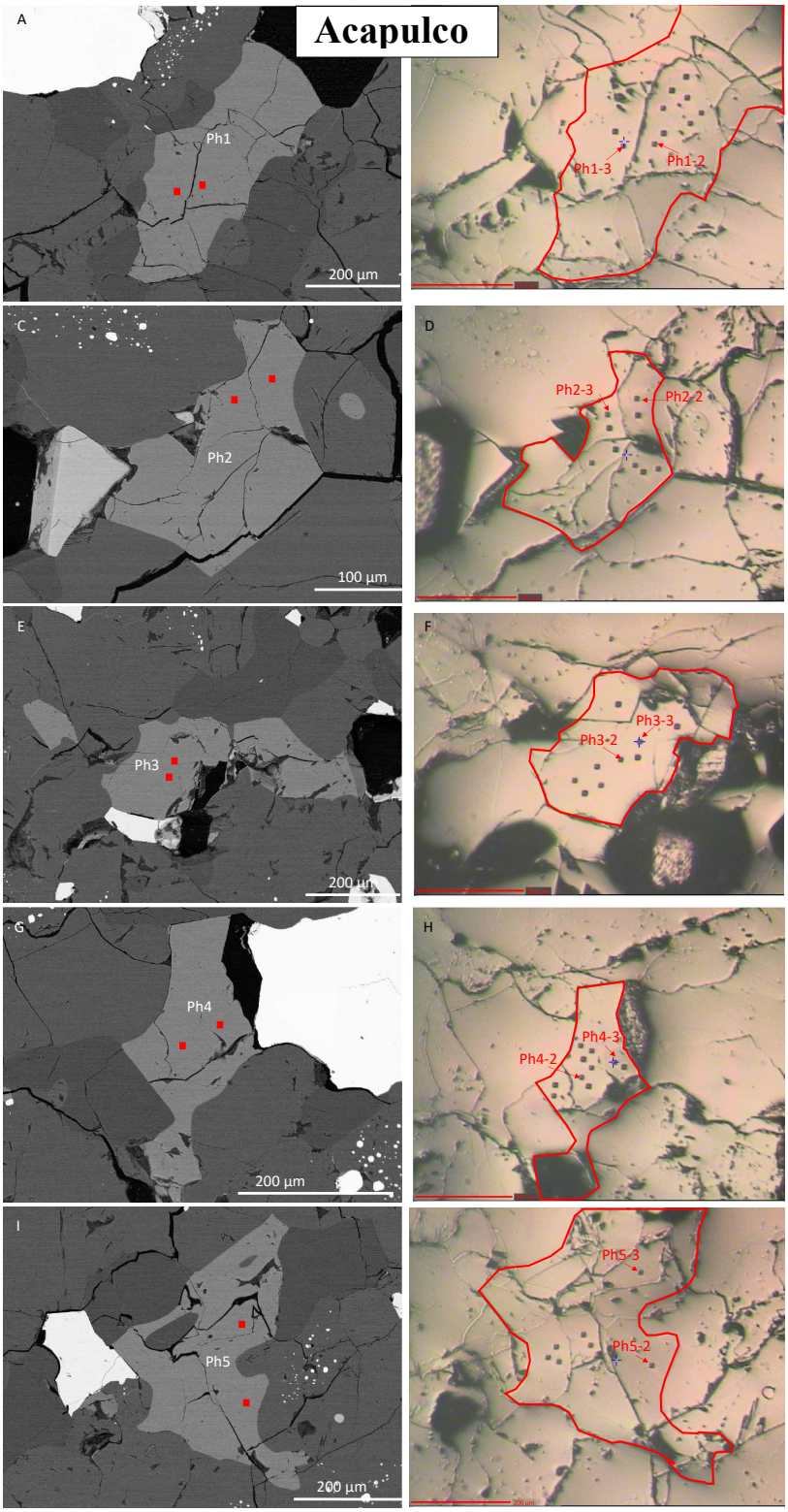
Acapulco
A
Ph1
200 µm
Ph1-3
Ph1-2
C
Ph2
100 µm
D
Ph2-3
Ph2-2
E
Ph3
200 µm
F
Ph3-3
Ph3-2
G
Ph4
200 µm
H
Ph4-3
Ph4-2
I
Ph5
200 µm
Ph5-3
Ph5-2

Figure S-2

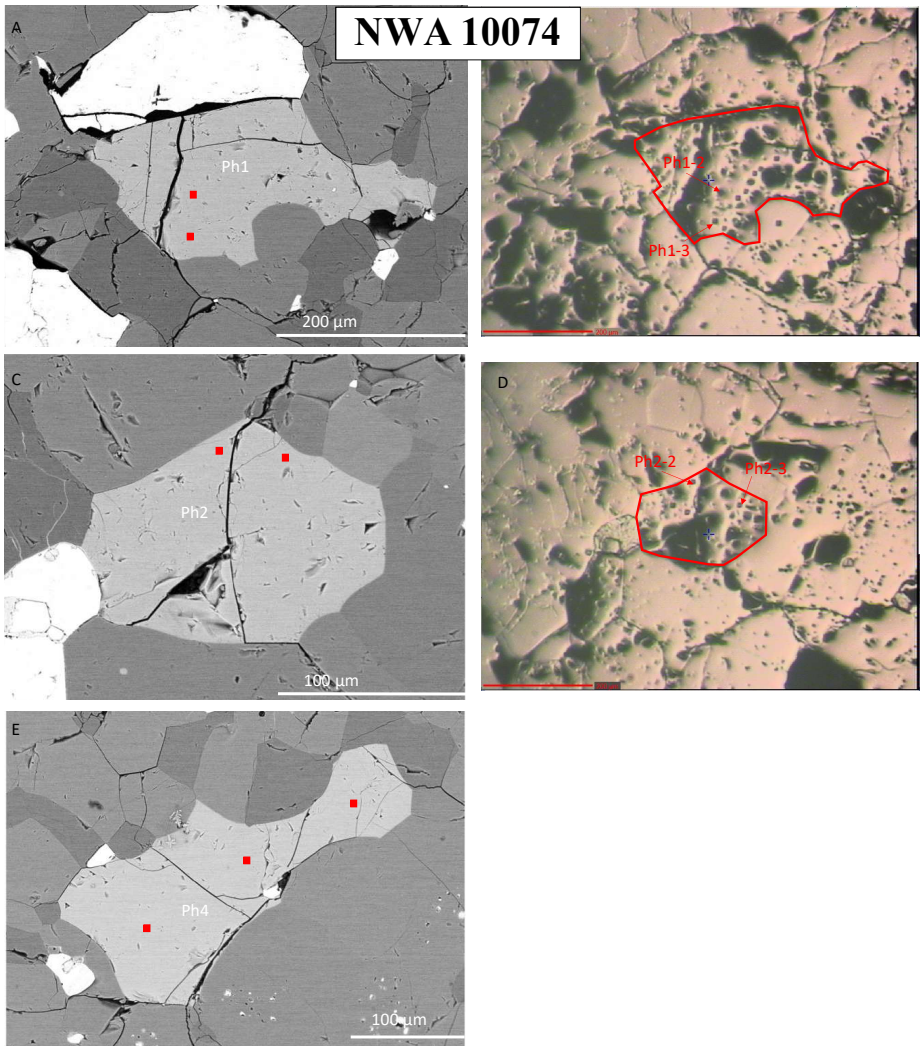

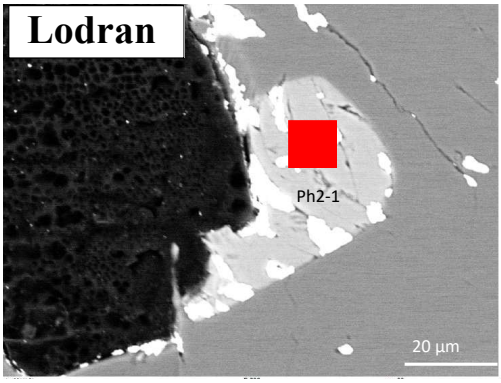

Figure S-2 *continued*

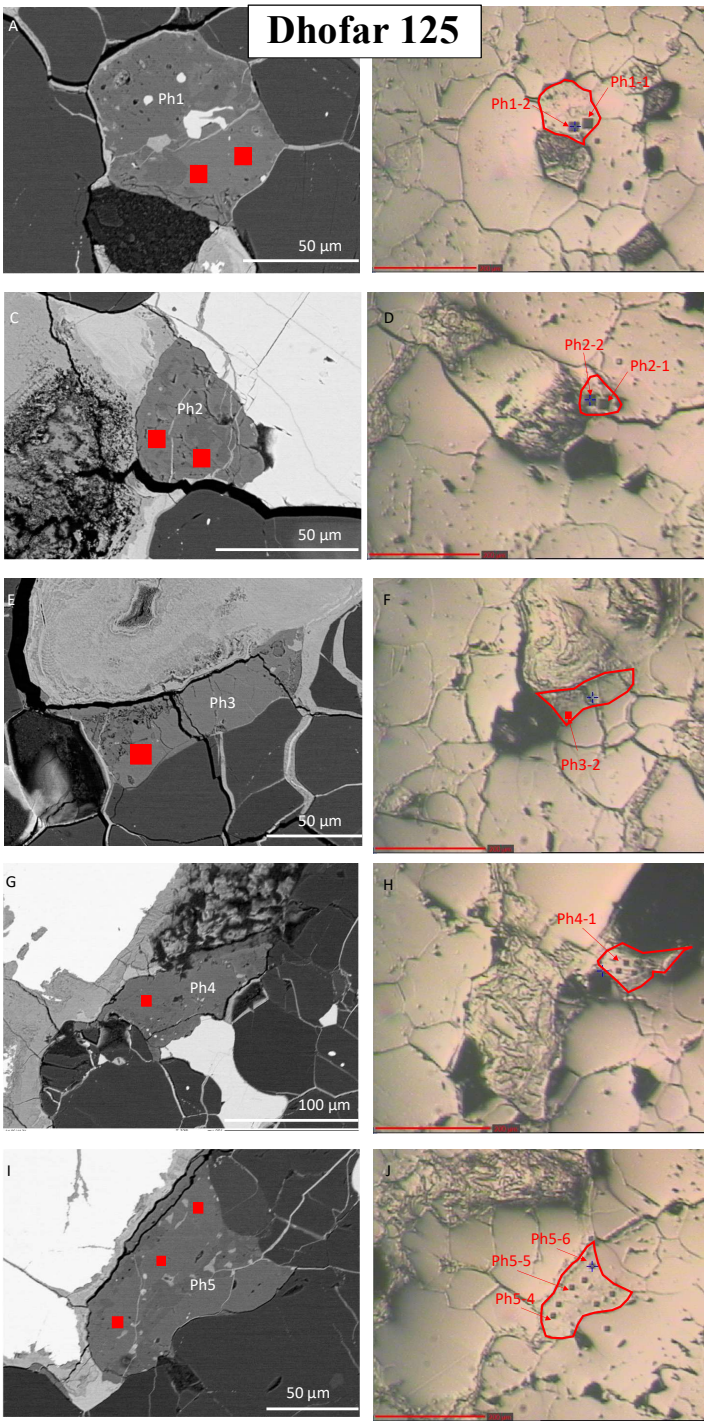

Figure S-2 BSE images of apatite and associated optical images highlighting the NanoSIMS spots. Extra spots appearing on the optical images were made for analytical settings and during hydrogen analyses (Stephant *et al.,* 2023).

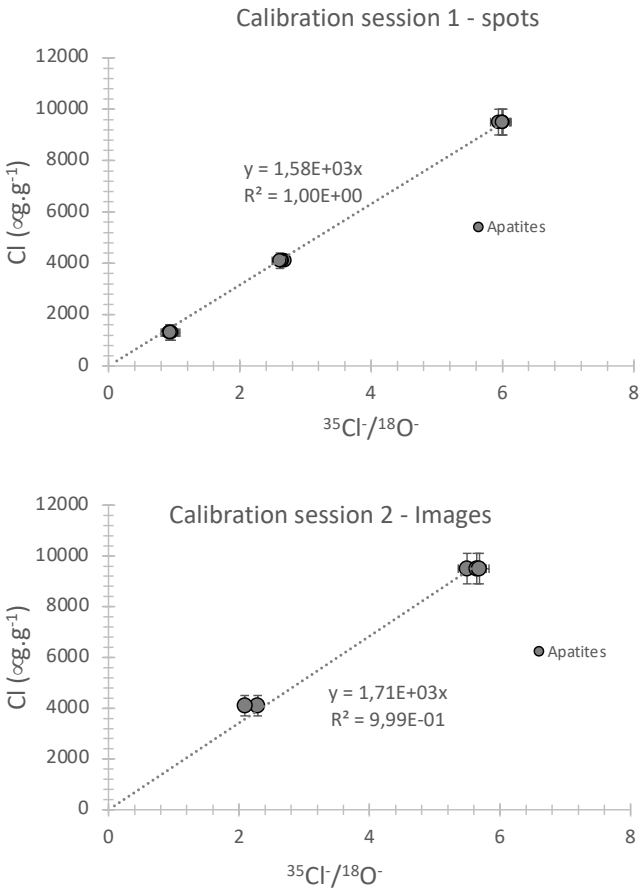

Figure S-3 Calibration curves for determination of chlorine abundance (μg.g^{-1}) as a function of $^{35}Cl^{-}/^{18}O^{-}$ measured by NanoSIMS based on terrestrial apatite standards.

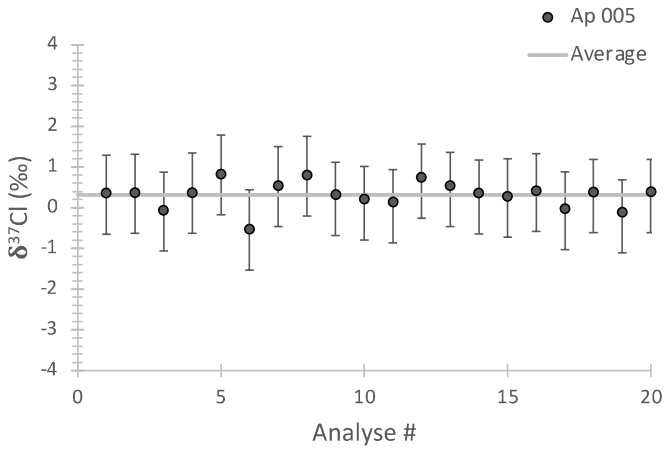

Figure S-4 Reproducibility of $\delta^{37}Cl$ in Apatite 005 standard over the duration of the analysis session. The error bars represent the analytical error associated within each measurement. Grey band represent the average $\delta^{37}Cl$ value of the standard.

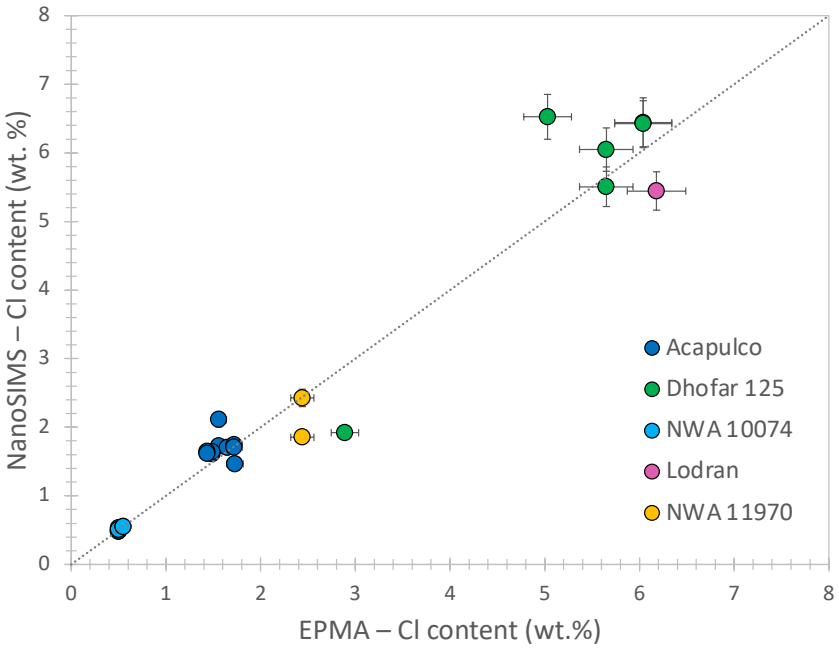

Figure S-5 EPMA *vs*. SIMS Cl abundances (wt. %) in acapulcoites and lodranites.

Supplementary Information References

Barnes, J.J., Tartèse, R., Anand, M., McCubbin, F.M., Neale, C.R., Franchi, I.A. (2016) Early degassing of lunar urKREEP by crust-breaching impact(s). *Earth and Planetary Science Letters* 447, 84–94. https://doi.org/10.1016/j.epsl.2016.04.036

Barrett, T.J., Barnes, J.J., Anand, M., Franchi, I.A., Greenwood, R.C., Charlier, B.L.A., Zhao, X., Moynier, F., Grady, M.M. (2019) Investigating magmatic processes in the early Solar System using the Cl isotopic systematics of eucrites. *Geochimica et Cosmochimica Acta* 266, 582–597. https://doi.org/10.1016/j.gca.2019.06.024

Christophe Michel-Levy, M., Lorin, J.C. (1978) El quemado, a new type of stone meteorite fallen near Acapulco (Abstract). *Meteoritics* 13, 411–412.

Davidson, J., Wadhwa, M., Hervig, R.L., Stephant, A. (2020) Water on Mars: Insights from apatite in regolith breccia Northwest Africa 7034. *Earth and Planetary Science Letters* 552, 116597. https://doi.org/10.1016/j.epsl.2020.116597

Davis, A.M., Prinz, M., Weisberg, M.K. (1993) Trace Element Distributions in Primitive Achondrites, *Lunar and Planetary Science Conference XXIV* 375-376, The Woodlands, Texas.

Garrison, D., Hamlin, S., Bogard, D. (2000) Chlorine abundances in meteorites. *Meteoritics and Planetary Science* 35, 419-429. https://doi.org/10.1111/j.1945-5100.2000.tb01786.x

Greyshake, A., Clayton, R.N., Mayeda, T.K. (2001) Dhofar 125: A new acapulcoite from Oman. *Lunar and Planetary Science Conference XXXII* #1325, The Woodlands, Texas.

Kaufman, R., Long, A., Bentley, H., Davis, S. (1984) Natural chlorine isotope variations. *Nature* 309, 338–340. https://doi.org/10.1038/309338a0

Ketcham, R.A. (2015) Technical Note: Calculation of stoichiometry from EMP data for apatite and other phases with mixing on monovalent anion sites. *American Mineralogist* 100, 1620–1623. https://doi.org/10.2138/am-2015-5171

Lanari, P., Vidal, O., De Andrade, V., Dubacq, B., Lewin, E., Grosch, E., Schwartz, S. (2014) XMapTools: a MATLAB©-based program for electron microprobe X-ray image processing and geothermobarometry. *Computers and Geosciences* 62, 227-240. https://doi.org/10.1016/j.cageo.2013.08.010

Lanari, P., Vho, A., Bovay, T., Airaghi, L., Centrella, S., (2019) Quantitative compositional mapping of mineral phases by electron probe micro-analyser. *Geological Society of London*, Special Publications 478, 39-63. https://doi.org/10.1144/SP478.4

Lanari, P., Laughton, J., Tedeschi, M., Markmann, T.A. (2023) XMapTools 4.1 (v4.1). *Zenodo.* https://doi.org/10.5281/zenodo.7656958

McCoy, T.J., Keil, K., Clayton, R.N., Mayeda, T.K., Bogard, D.D., Garrison, D.H., Huss, G.R., Hutcheon, I.D., Wieler, R. (1996) A petrologic, chemical, and isotopic study of Monument Draw and comparison with other acapulcoites: Evidence for formation by incipient partial melting. *Geochimica et Cosmochimica Acta* 60, 2681–2708. https://doi.org/10.1016/0016-7037(96)00109-3

McCoy, T.J., Keil, K., Clayton, R.N., Mayeda, T.K., Bogard, D.D., Garrison, D.H., Wieler, R. (1997a) A petrologic and isotopic study of lodranites: Evidence for early formation as partial melt residues from heterogeneous precursors. *Geochimica et Cosmochimica Acta* 61, 623–637. https://doi.org/10.1016/S0016-7037(96)00359-6

McCoy, T.J., Keil, K., Muenow, D.W., Wilson, L. (1997b) Partial melting and melt migration in the acapulcoite-lodranite parent body. *Geochimica et Cosmochimica Acta* 61, 639–650. https://doi.org/10.1016/S0016-7037(96)00365-1

McCubbin, F.M., Hauri, E.H., Elardo, S.M., Vander Kaaden, K.E., Wang, J., Shearer Jr, C.K. (2012) Hydrous melting of the martian mantle produced both depleted and enriched shergottites. *Geology* 40, 683-686. https://doi.org/10.1130/G33242.1

McCubbin F.M., Vander Kaaden K.E., Tartèse R., Boyce J.W., Mikhail S., Whitson E.S., Bell A.S., Anand M., Franchi I.A., Wang J.H., Hauri E.H. (2015) Experimental investigation of F, Cl, and OH partitioning between apatite and Fe-rich basaltic melt at 1.0-1.2 GPa and 950-1000 °C. *American Mineralogist* 100, 1790-1802. https://doi.org/10.2138/am-2015-5233

McCubbin, F.M., Lewis, J.A., Barnes, J.J., Elardo, S.M., Boyce J.W. (2021). The abundances of F, Cl, and H_2O in eucrites: Implications for the origin of volatile depletion in the asteroid 4 Vesta. *Geochimica et Cosmochimica Acta* 314, 270-293. https://doi.org/10.1016/j.gca.2021.08.021

Palme, H., Schultz, L., Spettel, B., Weber, H.W., Wänke, H., Michel-Levy, M.C., Lorin, J.C. (1981). The Acapulco meteorite: Chemistry, mineralogy and irradiation effects. *Geochimica et Cosmochimica Acta* 45, 727–752. https://doi.org/10.1016/0016-7037(81)90045-4

Papike, J.J., Spilde, M.N., Fowler, G.W., Layne, G.D., Shearer, C.K. (1995) The Lodran primitive achondrite: petrogenetic insights from electron and ion microprobe analysis of olivine and orthopyroxene. *Geochimica et Cosmochimica Acta* 59, 3061–3070. https://doi.org/10.1016/0016-7037(95)00195-6

Patzer, A., Hill, D.H., Boynton, W.V. (2004) Evolution and classification of acapulcoites and lodranites from a chemical point of view. *Meteoritics and Planetary Science* 39, 61–85. https://doi.org/10.1111/j.1945-5100.2004.tb00050.x

Stephant, A., Zhao, X., Anand, M., Davidson, J., Carli, C., Cuppone, T., Pratesi, G., Franchi, I.A. (2023) Hydrogen in acapulcoites and lodranites: A unique source of water for planetesimals in the inner Solar System, *Earth and Planetary Science Letters* 615, 118202. https://doi.org/10.1016/j.epsl.2023.118202

Tartèse, R., Anand, M., Joy, K.H., Franchi, I.A. (2014) H and Cl isotope systemat-ics of apatite in brecciated lunar meteorites Northwest Africa 4472, Northwest Africa 773, Sayh al Uhaymir 169, and Kalahari 009. *Meteoritics and Planetary Science* 49, 2266–2269. https://doi.org/10.1111/maps.12398

Yugami, K., Takeda, H., Kojima, H., Miyamoto, M. (1998) Modal mineral abundances and the differentiation trends in primitive achondrites. *Antarctic Meteorite Res*earch 11, 49–70.

Zipfel, J., Palme, H., Kennedy, A.K., Hutcheon, I.D. (1995) Chemical composition and origin of the Acapulco meteorite. *Geochimica et Cosmochimica Acta* 59, 3607–3627. https://doi.org/10.1016/0016-7037(95)00226-P